https://doi.org/10.5194/egusphere-2026-2684
Preprint. Discussion started: 13 July 2026

Evolution of the Auckland Volcanic Field (New Zealand) boundary

Craig A. Miller[1], James Muirhead[2], Emily J. Judd[3], Dougal Townsend[4], Angela L. Doherty[5], Jan Lindsay[2], and Graham Leonard[4]

[1]Earth Sciences New Zealand, Wairakei Research Center, Taupo, New Zealand
[2]University of Auckland, Auckland, New Zealand
[3]Earth Sciences New Zealand, Auckland, New Zealand
[4]Earth Sciences New Zealand, Avalon, Lower Hutt, New Zealand
[5]Auckland Emergency Management – Auckland Council, New Zealand

Correspondence: Craig A. Miller (craig.miller@earthsciences.nz)

Abstract. Monogenetic volcanic fields pose a significant risk to life and infrastructure when situated near urban regions. To place constraints on developing volcanic unrest scenarios and apply hazard mitigation measures, emergency planners and decision makers must consider where the next eruption may occur and the likelihood that it will be within the present bounds of the field. Utilising a high-precision chronology of eruptions, tested against a synthetically derived dataset, we examine the likelihood that the next eruption from the Auckland Volcanic Field (AVF) will occur within or outside of the present field boundary. We mapped the spatial-temporal growth of the field using a temporally evolving convex hull boundary, and the locations of subsequent eruptions were then tracked to test whether they fell within the convex hull boundary defined by the existing eruption centres. When considering eruptions since 63 ka, this retrospective approach reveals a probability of 71% that the next eruption will fall within the current boundary of the field or 74% when age uncertainty is considered. When a 3.5 km buffer is added to the convex hull, the probability increases to 98%. Meanwhile, use of a synthetic dataset allows a forward looking analysis which suggests a 2 km buffer may be sufficient to capture at least 95% of future eruption locations. We found that the AVF boundary grew in steps, where one to four new eruptions would occur outside the boundary with subsequent eruptions within the newly expanded boundary. Local scale spatio-temporal clustering also occurs with successive clustered centres aligning in a NNE/NE direction. We propose that this process relates to either changing magmatic source processes or crustal magmatic pathways that are available for use for multiple eruptions before closing off to new magma due to conduit cooling, solidification or changing tectonic stress patterns.

1 Introduction

Monogenetic volcanic fields (Németh and Kereszturi, 2015; Smith and Németh, 2017) are a common form of volcanism found in many tectonic settings and occur on every continent (Cañón-Tapia, 2016). The number of eruptive centres in these fields varies from tens to thousands and spatial extents from hundreds to thousands of square kilometers (Global Volcanism Program, 2025-11-26, 2025). Their ubiquity and wide spatial extent mean that many volcanic fields inevitably overlap with population centres and critical infrastructure (e.g., Chichinautzin Volcanic Field, Mexico City Torres et al., 2023), requiring them to be assessed and managed as an important hazard (Marrero et al., 2019; Ang et al., 2020).

https://doi.org/10.5194/egusphere-2026-2684
Preprint. Discussion started: 13 July 2026

The distribution of volcanic centres within monogenetic fields is either random or clustered, reflecting underlying magma sources and crustal structural controls (Le Corvec et al., 2013b; Martí et al., 2016; Dahm et al., 2020; Cañón-Tapia, 2023). As a result, the extent or boundary of monogenetic fields may also show alignment with underlying structures (Tadini et al., 2014; Mazzarini et al., 2016). Defining the extent and shape of the field is challenging (Runge et al., 2015), but is important because it is often interpreted as reflecting the extent of the underlying magma source (Spörli and Eastwood, 1997; Brenna et al., 2012; Zhang et al., 2025). In younger fields, with the potential for future eruptions, a commonly asked question is: 'where will the next eruption take place?' In fields with apparently random volcanic vent distributions it is challenging to answer this question with any certainty, although numerous models have been proposed (e.g. Connor et al., 1992; Magill et al., 2005; Bebbington and Cronin, 2011; Martí et al., 2016; Mazzarini and Isola, 2024; Bebbington et al., 2025). By contrast, in fields with strong structural alignment narrower corridors of likelihood can be defined (Runge et al., 2014), although individual vent locations cannot be predicted.

Here we pose a fundamental question that holds value for emergency management officials tasked with managing volcanic hazards in monogenetic fields: 'What is the likelihood of the next eruption centre being within the existing field boundary?' We consider this problem for the Auckland Volcanic Field (AVF) in New Zealand, where the answer to this question is particularly significant for Auckland Emergency Management and Auckland Council given that the field is located in the metropolitan centre of Auckland (Hopkins et al., 2021; Lindsay et al., 2026), a city with a population of over 1.7 million people. Determining whether the next eruption is more likely to be inside or outside of the current boundary places useful constraints on the development of eruption scenarios (e.g. Hayes et al. 2018; Hayes et al. 2020), and in the provision of science advice support to develop response and evacuation plans (Auckland Council, 2024; Auckland Emergency Management, 2024).

The AVF also provides a globally unique case study for examining this question, as 94 % of the eruptive centres have an associated eruption age (Hopkins et al. 2021). Using this recently updated dataset of eruption ages we present a brief analysis of the evolution of the AVF boundary and adopt a method to examine the likelihood of the next eruption occurring within the existing boundary of the field. These results are compared with synthetically derived datasets of eruptive centre locations to test how these likelihoods vary as a function of the field boundary size and number of eruptive centres.

1.1 Extent of the Auckland volcanic field

The AVF consists of at least 54 volcanic centres (Figure 1) that appear to be randomly located (Le Corvec et al., 2013a), and range in eruptive volume from 0.008 to 1851 x 10^7 m^3 (Kereszturi et al., 2013), displaying both explosive and effusive eruptive styles (Allen and Smith, 1994). For this study we consider eruptive centres rather than eruptive events, noting that is is possible that some centres may have had more than one period of eruptive activity, such as Rangitoto, which has had two distinct phases of activity (Needham et al., 2011), separated by a 50 year or greater time gap (Shane et al., 2013; Linnell et al., 2016; Allington et al., 2023). The AVF is relatively small ($\sim$ 374 km^2) with moderate to high vent density (0.14 vents km^{-2}; Le Corvec et al., 2013b). The youngest and largest eruption (Rangitoto [51]) extended the previous extent of the field to the northeast.

https://doi.org/10.5194/egusphere-2026-2684
Preprint. Discussion started: 13 July 2026

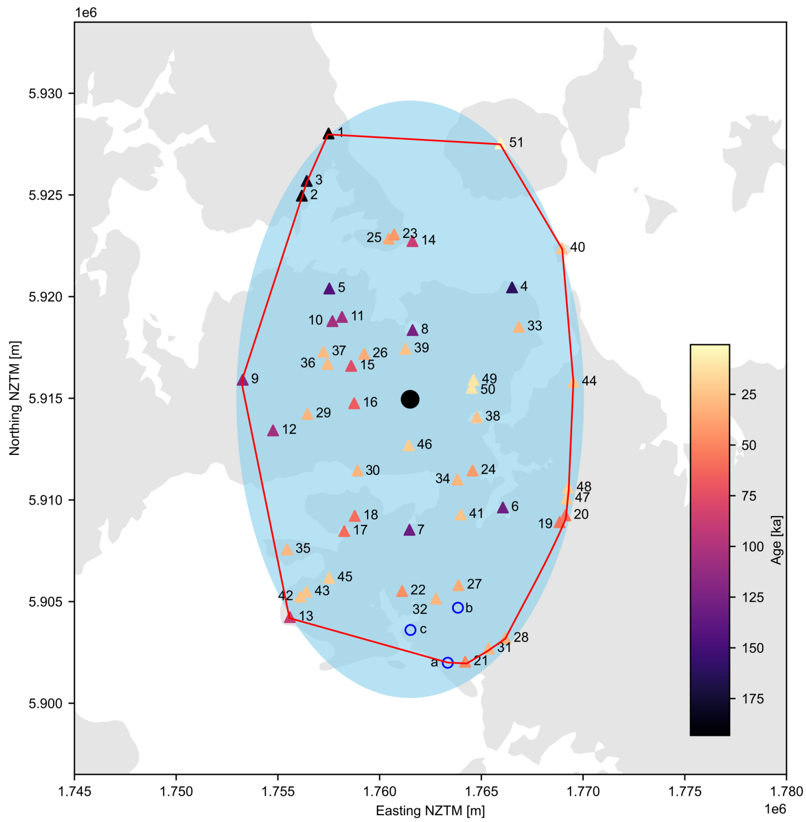

Figure 1. Locations of the eruption centres in the Auckland Volcanic Field colour coded by age Hopkins et al. (2021). The blue circles are eruptive centres that do not have an age date. The filled blue ellipse representing the field extent is defined by the parameters in Spörli and Eastwood (1997), while the red line is the convex hull. The black dot marks the centre point of the ellipse. Eruption centres are numbered according to their age rank from oldest to youngest. 1) Pupuke Moana [193.2 ka], 2) Te Kopua-o-Matakerepo/Onepoto [187.6 ka], 3) Te Kopua-o-Matakamokamo/Tank Farm/Tuff Crater [181 ka], 4) Whakamuhu/ Glover Park/St Heliers Volcano [161 ka], 5) Albert Park Volcano [145 ka], 6) Pukewairiki/Highbrook Park [130 ka], 7) Boggust Park Crater [130 ka], 8) Ōrākei Basin [126 ka], 9) Te Ahi-kā-a-Rakataura/Ōwairaka/ Mt Albert [119.2 ka], 10) Grafton Volcano [106.5 ka], 11) Pukekawa/Auckland Domain [106 ka], 12) Puketāpapa/ Pukewīwī/ Mt Roskill [105.3 ka], 13) Maungataketake/Elletts Mountain [88.9 ka], 14) Maungauika/North Head [87.5 ka], 15) Te Kōpuke/Tītīkōpuke/ Mt St John [75.3 ka], 16) Maungakiekie/One Tree Hill [67 ka], 17) Māngere Lagoon [59.5 ka], 18) Te Pane-o-Mataaho/Māngere Mountain [59 ka], 19) Hampton Park Volcano [57 ka], 20) Te Puke-o-Taramainuku/Ōtara Hill [56.5 ka], 21) Matukutūreia/McLaughlins Mountain [48.2 ka], 22) Te Pūkaki Tapu-o-Poutukeka/Pūkaki Lagoon [45 ka], 23) Takararo/Mt Cambria [42.3 ka], 24) Te Apunga-o-Tainui/McLennan Hills [41.3 ka], 25) Takarunga/Mt Victoria [34.8 ka], 26) Ōhinerangi/Mt Hobson/Ōhinerau [34.2 ka], 27) Kohuora Crater [33.7 ka], 28) Ash Hill Crater [31.8 ka], 29) Te Tātua-a-Riukiuta/Three Kings [31 ka] , 30) Te Hopua-a-Rangi/Gloucester Park [31 ka], 31) Te Manurewa-o-Tamapahore/Matukutūruru/ Wiri Mountain [30.5 ka], 32) Crater Hill [30.4 ka], 33) Taurere/Taylors Hill [30.2 ka], 34) Ōtāhuhu/Mt Richmond [30.2 ka], 35) Te Motu-a-Hiaroa/Puketūtū [29.4 ka], 36) Te Pou Hawaiki [28 ka], 37) Maungawhau/Mt Eden [28 ka], 38) Te Kopua Kai-a-Hiku/Panmure Basin [25.2 ka], 39) Maungarahiri/Little Rangitoto [24.6 ka], 40) Motukorea/Browns Island [24.4 ka], 41) Mt Robertson/Sturges Park [24.3 ka], 42) Ōtuataua [24.2 ka], 43) Puketapapakanga-a-Hape/Pukeiti [23.7 ka], 44) Ōhuiarangi/Pigeon Mountain [23.4 ka], 45) Moerangi/Waitomokia/Mt Gabriel [20.3 ka], 46) Rarotonga/Mt Smart [20.1 ka], 47) Matanginui/Green Mount [19.6 ka], 48) Styaks Swamp Crater [19.1 ka], 49) Te Tauoma/Purchas Hill [10.9 ka], 50) Maungarei/Mt Wellington [10.0 ka], 51) Rangitoto [0.504 ka], a) Cemetery Crater [undated] b) Puhinui Craters [undated] c) Un-named. [undated]

https://doi.org/10.5194/egusphere-2026-2684
Preprint. Discussion started: 13 July 2026

Several methods have been proposed to define the shape of the AVF boundary depending on the purpose of the research. An elliptical boundary (Figure 1) was fitted to outer vent locations by Spörli and Eastwood (1997) and interpreted to correspond to an elliptical magma source area in the lithospheric mantle. An outer buffer ellipse that has twice the area of the inner boundary ellipse, was used by Bebbington (2013) for spatio-temporal hazard models, while Le Corvec et al. (2013b) used a convex hull with a 1 km buffer for a study of the spatial, temporal and chemical evolution of the field. A rectangular boundary was used by Lindsay et al. (2010) for a Bayesian event tree analysis applied to eruption forecasting, where a regular grid-/cell-based model was required. Runge et al. (2015) analysed the sensitivity of the boundary geometry for hazard assessment and concluded that, for the AVF, different options created similar shapes, but for some statistical tests there was substantial variation in results depending on boundary shape.

With no strong indication of where the next eruption will occur, emergency management officials must consider that a future eruption could occur anywhere within the current field boundary. They must also take into account the possibility that the next eruption could occur outside the boundary of the current field. A 5 km buffer for the AVF was proposed by Runge et al. (2015), based on analysis of the Harrat Rahat volcanic field in Saudi Arabia, drawing on probabilistic analysis of dyke length and expert elicitation (Runge et al., 2014). This 5 km buffer around the ellipse defining the AVF boundary of Spörli and Eastwood (1997); Hayes et al. (2018) accounts for our current scientific uncertainty and is used to inform emergency management response and evacuation planning.

Here we examine the change of the AVF boundary over time, using the convex hull method, which does not presume any particular geometric shape and provides a minimum bounding extent. There is only a small difference between the bounding ellipse and the present-day convex hull (Figure 1), mostly in the north and south which slightly impacts the extent of buffer distances. An animated illustration of the AVF growth is presented in supplementary material (REF). In this manuscript we prefer the use of the te reo Māori names for volcanoes and the number given in square brackets '[1]' after the name refers to the eruption order illustrated in Figure 1, which also has the English name.

1.2 Chronology of eruptive centres

The field boundary shape evolution over time is dependent on the correct age ordering of centres within the field. We use the chronology presented in Hopkins et al. (2021) as the most reliable source of modern age date information for the AVF, which updates previous age compilations of Lindsay et al. (2011); Bebbington and Cronin (2011); Leonard et al. (2017) (Figure 2). Compared to other volcanic fields globally, the AVF is uniquely positioned for our analysis owing to the nearly complete dataset of volcanic centre ages.

https://doi.org/10.5194/egusphere-2026-2684
Preprint. Discussion started: 13 July 2026

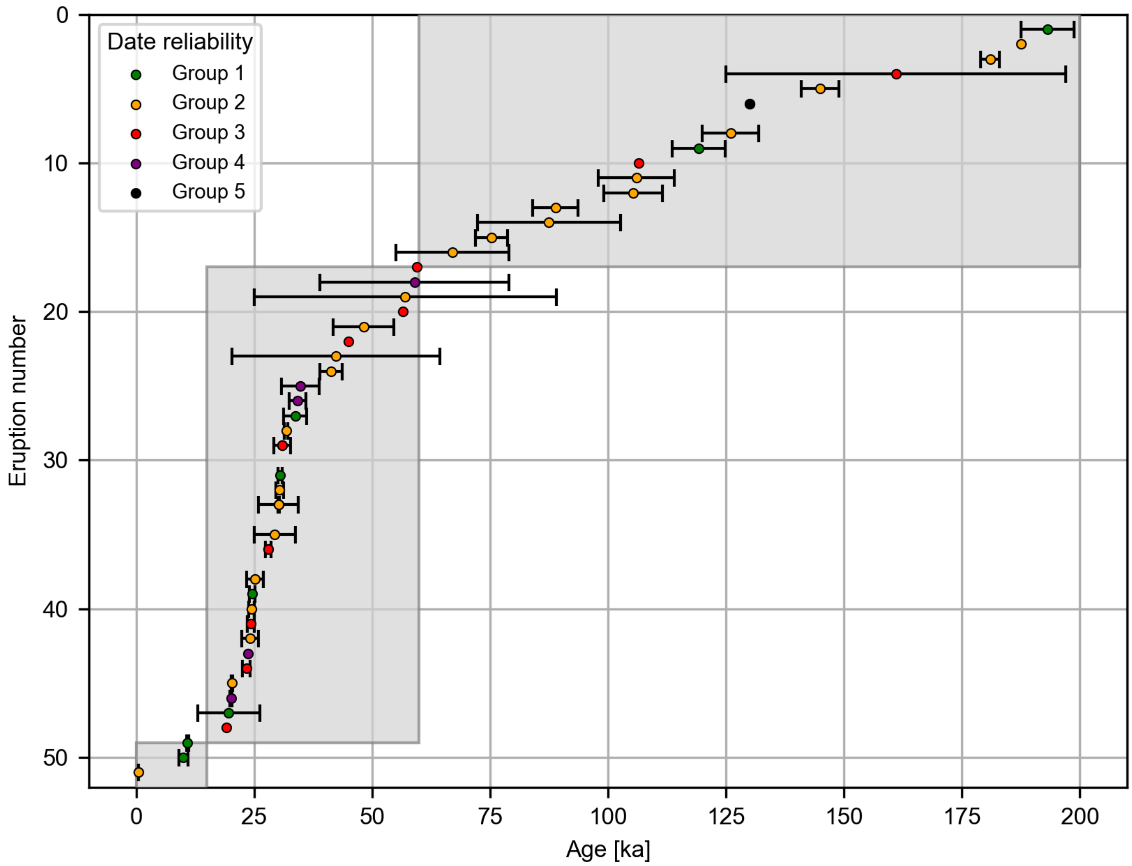

Figure 2. AVF eruption ages (error bars are 2 standard deviations) plotted as a function of eruption age (ka) and coloured by date reliability group. The grey boxes show three time ranges characterised by different growth rates of the field described in Hopkins et al. (2021). Figure modified from Hopkins et al. (2021).

Fifty-one AVF volcanic centres are dated directly or indirectly, while the three most recently discovered (Cemetery Crater, Puhinui Craters and an unnamed eruption centre) currently have no age estimate (blue circles in Figure 1). Of those directly dated, usually with $^{40}Ar/^{39}Ar$ or ^{14}C dates, errors range from 10 years (Rangitoto) to 32,000 years (Hampton Park Volcano). Pukewairiki [6] and Boggust Park Crater [7] are given the same minimum ages (>130 ka) and hence have uncertain date order.

Hopkins et al. (2021) defined five categories of date reliability: Group 1 - reliable reproducible ages (9 centres); Group 2 - reliable single age determinations, several reliable ages spanning a small range, or strong paleomagnetic correlations to well dated centres (25 centres); Group 3 - ages based on tephrochronology or sedimentation rates in drill cores (11 centres); Group 4 - varied or conflicting age determinations (5 centres); Group 5 - no direct or minimum age determined (1 centre).

https://doi.org/10.5194/egusphere-2026-2684
Preprint. Discussion started: 13 July 2026

The eruption rate and mean eruptive repose period of the field have varied over time and can be divided into three periods (Leonard et al., 2017; Hopkins et al., 2021), shown as shaded boxes in Figure 2. The first period, categorized as an initial slow growth period, includes 16 eruptions, spanning from the first eruption at 193 ka (Pupuke Moana [1]) to 67 ka (Maungakiekie [16]). The second period, marked by rapid growth includes 32 eruptions between 59 ka (Mangere Lagoon [17]) and 19 ka (Styaks Swamp Crater [48]). The third period, which ranges between 11 ka and present day, contains only 3 eruption centres (Te Tauoma [49], Maungarei [50] and Rangitoto [51]). However, the volume of erupted material in the last eruption(s) at Rangitoto, exceeds the volume from the rest of the field combined.

2 Methods

2.1 Field area growth

Using the eruption order from Hopkins et al. (2021) and centre coordinates from QMAP (Heron, 2023), we computed the convex hull of the field across the evolution of the AVF. After the first three eruptions a convex hull polygon is formed and we can then assess whether the 'next' (i.e., 4th) eruption occurs inside or outside the boundary of the hull. We redraw the boundary for each subsequent eruption and again assess if the next eruption centre occurs inside or outside the boundary. Repeating this process produces a sequence of convex hull geometries and a binary flag indicating whether each eruption centre was located inside or outside the preceding convex hull.

We use changes in spatial centrality of eruption centres within the convex hull over time to explore patterns of field growth. The Tukey depth is a measure of how central a point is within a multivariate point cloud and is determined by the smallest number of data points contained in any convex hull that includes the point (Tukey, 1975). Eruption centres with a high Tukey depth are those lying within the core of the field, while those with a low Tukey depth mark the expanding edges of the field.

We can summarise the present-day eruption centre distribution using a Tukey 'bag plot' (Rousseeuw and Ruts, 1999). The 50% depth region (the 'bag') is defined as the convex hull of the deepest half of the eruptions centres when ranked by Tukey depth. It should not be interpreted as containing 50% of the eruption centres alone, only when ranked by their Tukey depth. It can be thought of as representing the smallest convex region that contains the 'deepest' i.e. most central, portion of the eruption centres. The 'fence' is obtained by radially expanding the bag away from the Tukey median by a factor of three. Points outside the fence can be viewed as outliers.

2.2 Synthetic dataset

To contextualise our results, and examine the likelihood of future eruptions occurring within the present field boundaries, we developed a synthetic dataset comprising 1,000 simulations, each containing 250 randomly distributed volcanic centres. For each simulation, a sequence of vent locations was randomly generated within a bounding ellipse defined by the parameters of Spörli and Eastwood (1997). If, as proposed by Spörli and Eastwood (1997), this ellipse represents a long-term magma source at depth, then there is a physical justification for this being close to a maximum extent. After each successive eruption, we

https://doi.org/10.5194/egusphere-2026-2684
Preprint. Discussion started: 13 July 2026

determined: [1] the convex hull geometry, [2] whether the current eruptive centre was located within the preceding hull, [3] the distance to the hull boundary, when the centre was outside of the previous hull, [4] the area ratio, defined as the area of the current convex hull divided by the area of the bounding ellipse, and [5] the Euclidian distance between successive eruption centres. To test how sensitive our results are to the choice of bounding ellipse size, we repeated the processes adding both a 2km and 5km buffer to the ellipse (Appendix Figure A1).

2.3 Clustering and alignments

To determine the extent to which eruption centres within the AVF are spatiotemporally clustered, we computed the Euclidian distance and azimuth between successive vents. Euclidian distances were also computed for successive vents from our synthetic model, representing the null hypothesis that vents are randomly distributed. Results from these analyses allow us to identify successive eruptive centres in the AVF that exhibit anomalously high clustering and the azimuthal angles provide insight into potential structural alignments formed by either feeder dikes or pre-existing structures controlling magma ascent (e.g. Le Corvec et al., 2013b)

2.4 Eruption location probability relative to the field boundary

Whether the next eruption will occur within the current bounding ellipse of the AVF remains a central question for hazard assessment and mitigation. We estimate this probability using four approaches: [1] geological data with deterministic chronologies, [2] geological data with bootstrapped chronologies, [3] leave-one-out resampling, and [4] the synthetic dataset.

The first approach is to calculate the fraction of past AVF eruptions that occurred within the convex hull defined by all older vents, using the chronology produced from the preferred reported age of each vent. The second approach uses the same method as the first, but incorporates chronological uncertainty by iteratively (N = 10,000) generating alternative eruption chronologies by resampling eruption ages from a uniform distribution bounded by their reported minimum and maximum ages (and assigning a 5000-year uncertainty where none is available). The third approach, leave-one-out, utilises the same geological dataset but disregards the eruption order; eruption centres are systematically removed, and we test whether the omitted centre(s) fall within the convex hull defined by the remaining vents. All 51 permutations were computed. Finally, the fourth approach utilises the probabilities derived from the synthetic dataset by quantifying the proportion of synthetic eruptions that fall within the convex hull as a function of eruptive count.

2.5 Buffer distance and probability

We explore the relationship between buffer size and the probability that the next eruption occurs within that expanded convex hull using the deterministic and bootstrapped geological data, leave-one-out analyses, and synthetic dataset. For each scenario described below, we evaluate 25 buffer sizes, ranging from 0 to 12 km in fixed 500 m increments.

In each scenario and time step, a buffer is added to the convex hull and we determine whether the subsequent eruption falls within the buffered hull. Probabilities are defined as the proportion of eruptions captured within the buffered hull across the

https://doi.org/10.5194/egusphere-2026-2684
Preprint. Discussion started: 13 July 2026

temporal extent of the field. The first scenario considers all vents and uses the median reported ages for each vent (Figure 2). The second scenario only includes results from vents younger than 63 ka (N=35), which marks a behavioural shift in the field (Figure 2) (Hopkins et al., 2021). To account for uncertainty in the eruption chronology, we include two additional scenarios utilising the bootstrapped age models.

For the leave-one-out analysis, we calculate the proportion of withheld eruptions whose distance to the convex hull is less than or equal to each buffer threshold. As with the geological scenarios, we also include a scenario restricted to permutations that contain only the 35 youngest vents. For the synthetic dataset, we evaluate the buffer-to-probability relationship at t=52 (i.e., the 'next' eruption within the AVF) using the same approach as the leave-one-out analysis.

3 Results

3.1 Field area growth

Since the inception of the AVF, the complexity and area of the convex hull have both progressively increased (Figure 3) as new centres erupt outside the previous hull (Figure 4).

The area of the convex hull at present is 335 km^2 compared to 374 km^2 for the best-fit bounding ellipse area of Spörli and Eastwood (1997) (Figures 1, 3D). Since ∼125 ka, the areal growth of the field has occurred in a step-wise fashion where the field goes through periods of eruptions occurring exclusively within the convex hull followed by one to four eruptions outside the hull, then a renewed period of eruptions exclusively inside the new convex hull, and so forth (Figure 4). For example, following the formation of the first convex hull (after the eruptions of Pupuke Moana [1], Te Kopua-o-Matakerepo [2] and Te Kopua-o-Matakamokamo [3]), the next four eruptions Whakamuhu [4], Albert Park Volcano [5], Pukewairiki [6] and Boggust Park Crater [7]) between 145 ka and 130 ka all occurred outside the preceding hull (Tukey depth = 1), expanding the area from 38 to 117 km^2. Ōrākei Basin [8] (126 ka) was the first eruption to fall within the previous convex hull (Figure 3). Similarly, between 57 and 48 ka Hampton Park Volcano [19], Te Puke-o-Taramainuku [20] and Matukutūreia [21] formed outside the prior convex hull and expanded the field area from 209 km^2 to 274 km^2. From 48 to 24 ka, the field only expanded from 274 km^2 to 278 km^2 with 16 out of 18 eruptions occurring inside a previous convex hull. At 24 ka the eruption of Motukorea [40] expanded the area of the convex hull from 278 km^2 to 315 km^2. The field extent stayed constant at this area until the emergence of Rangitoto [1] volcano (via at least 2 eruptions around 600 years ago) expanded the boundary to its present extent.

This stepped field area growth is also shown by the Tukey depth over time as the field evolves (Figure 4). Up to 48 ka the field mostly grew by expanding its boundaries (Tukey depth=1), with 12 out of 21 eruption centres occurring outside the convex hull at the time of their formation. Between 45 ka and 10 ka the field oscillated between periods of eruption centres infilling the convex hull (high depth score) and expansion of the hull (depth =1). The cluster of events around 25 ka were deep within the existing hull boundary.

https://doi.org/10.5194/egusphere-2026-2684
Preprint. Discussion started: 13 July 2026

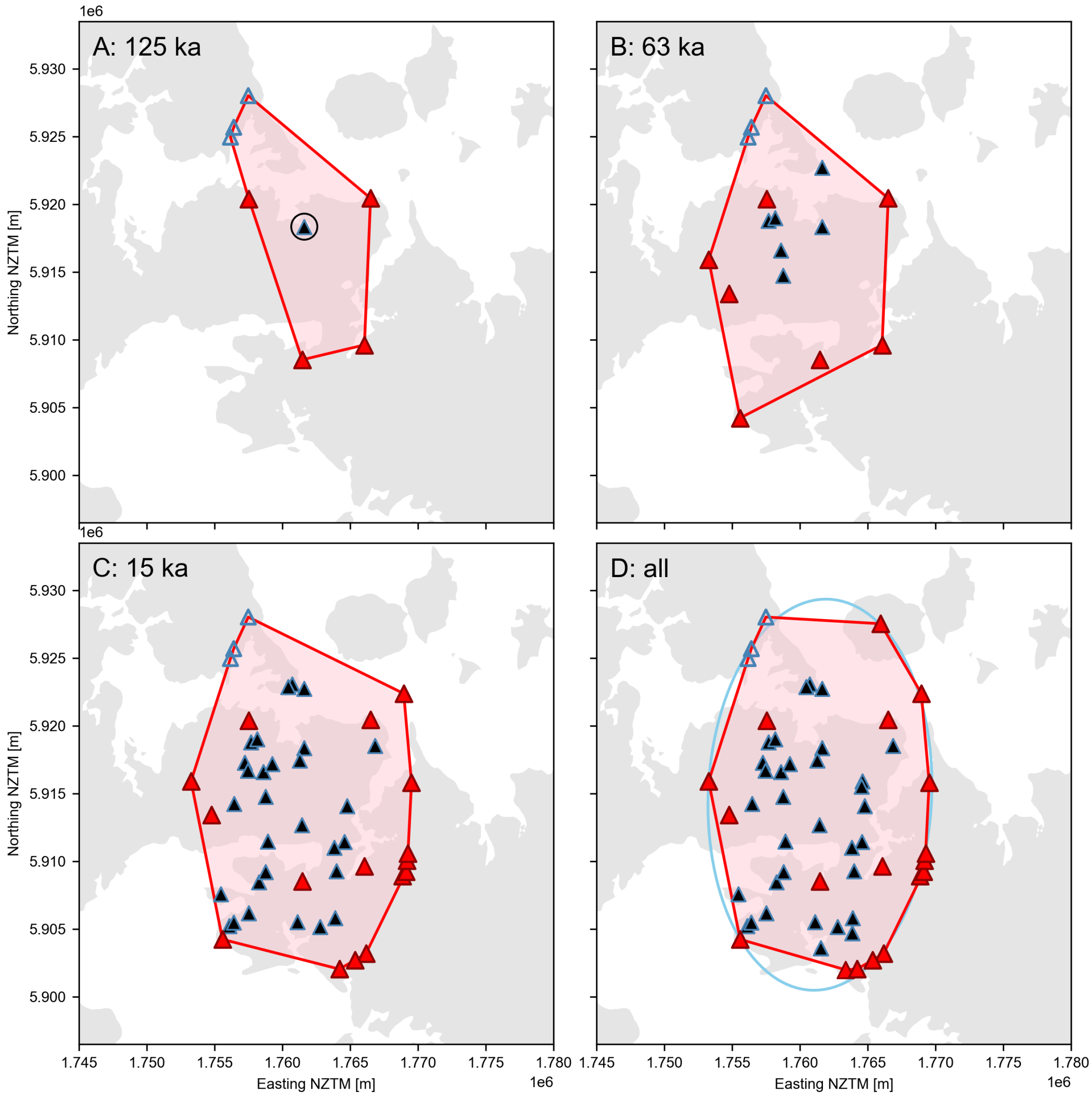

Figure 3. Calculated AVF convex hull at four time stamps showing its growth with time. Black triangles represent eruptive centres that erupted within the convex hull that existed at the time of their formation, whilst red triangles are those eruption centres that erupted outside the convex hull that existed at their time of formation. The first three eruptions required to make the first convex hull are shown as unfilled triangles. A) At 125 ka, when the first centre (Ōrākei Basin - circled) occurred inside the convex hull. B) At 63 ka, representing the convex hull at the end of the "slow growth" period. C) At 15 ka, representing vents at the end of the "fast growth" period. D) Present day, with the outline ellipse from Figure 1 shown for comparison.

https://doi.org/10.5194/egusphere-2026-2684
Preprint. Discussion started: 13 July 2026

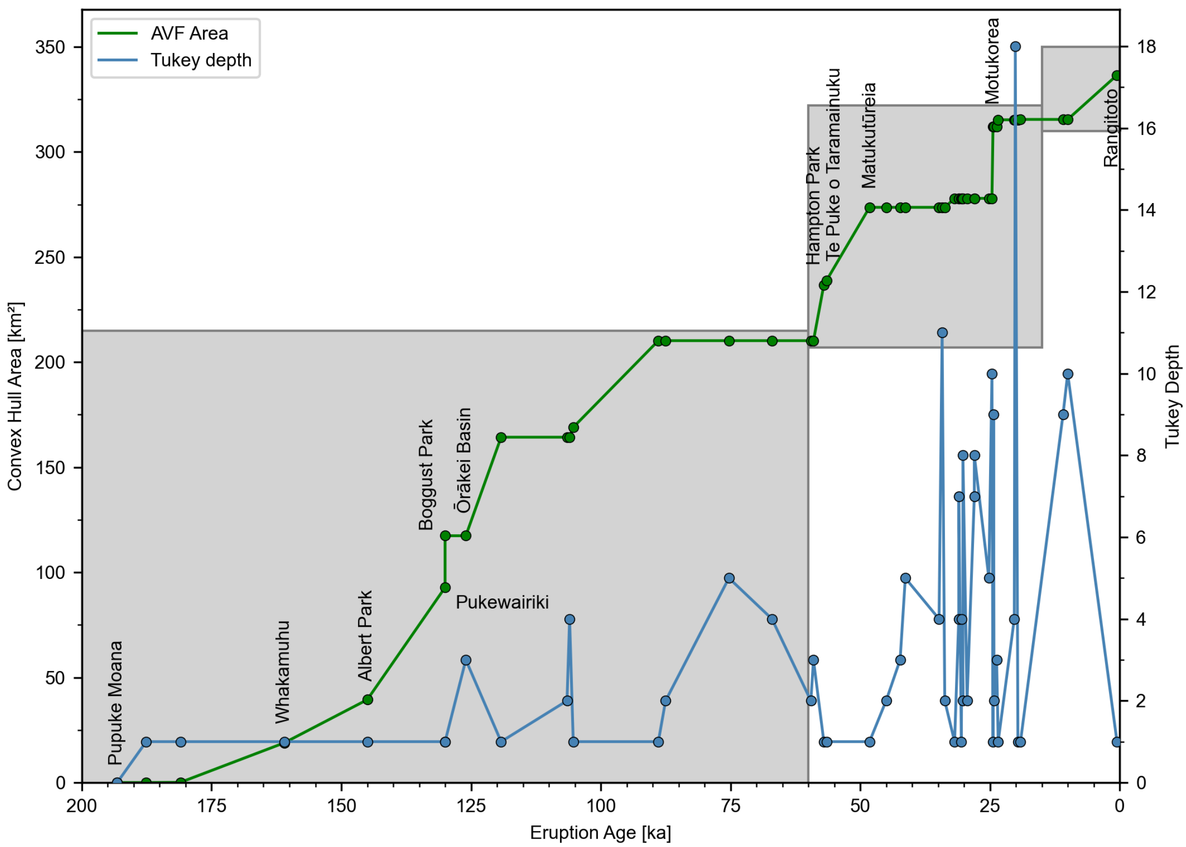

Figure 4. Evolution of the area of the AVF (green line) taken from the convex hull of the centre locations with no buffer added. The Tukey depth is shown in the blue line. Note the x axis is ordered from oldest (left) to youngest (right). The shaded boxes are the growth periods from Figure 2.

Results from the analysis of spatial centrality show there are 11 eruption centres within the 'bag' region (Figure 5). The median is the centre of the AVF and is coincident with Rarotonga [46]. We see that both the oldest centre (Pupuke Moana) and the youngest (Rangitoto) are outliers, as are Motukorea and a cluster of centres in the southwest. To the east and south the fence extends 1 to 2 km past the centres on the periphery of the field.

https://doi.org/10.5194/egusphere-2026-2684
Preprint. Discussion started: 13 July 2026

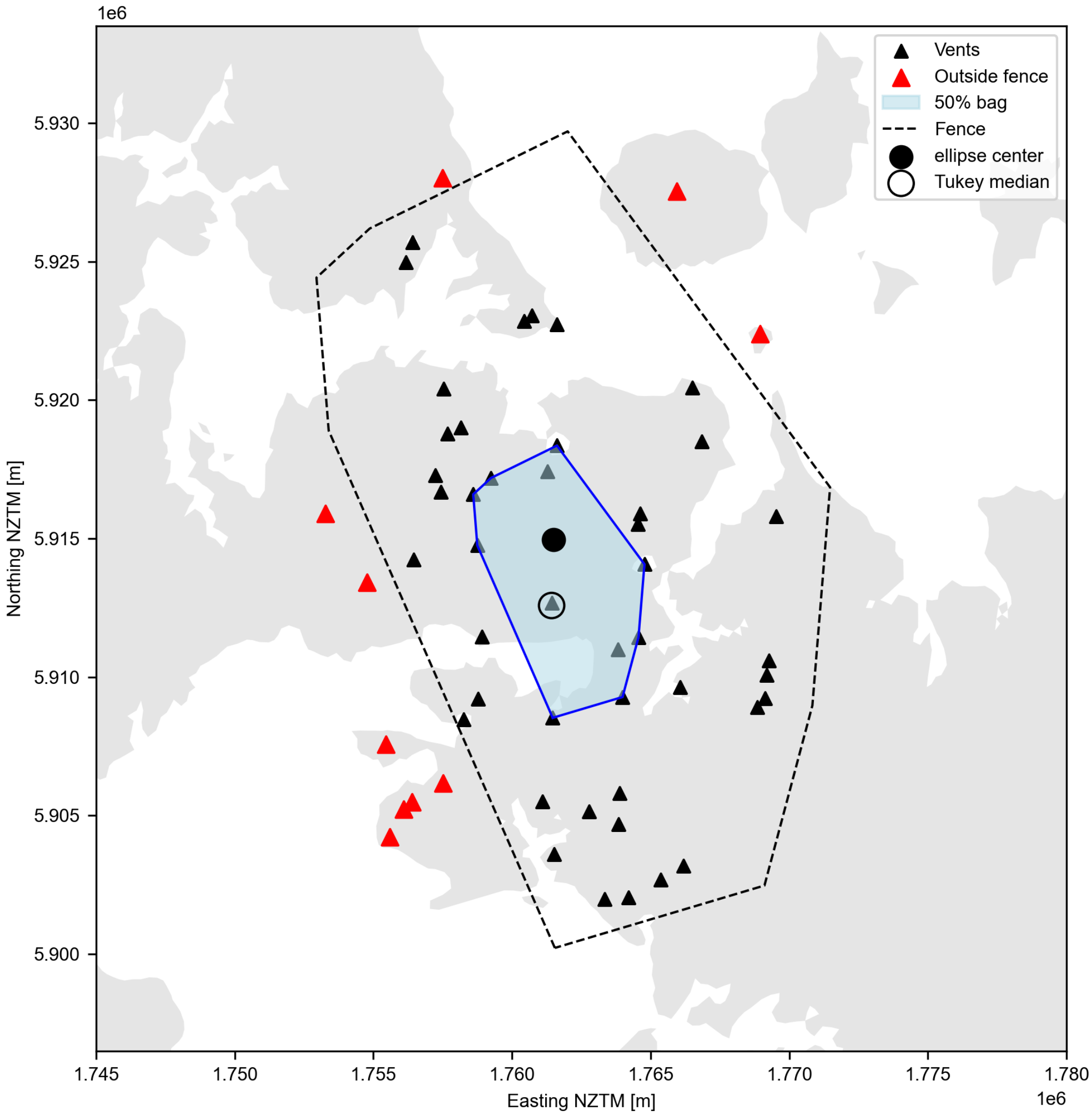

Figure 5. Bag plot of AVF vent distribution. The unfilled black circle represents the median point, and the filled black circle is the centre of the AVF from the elliptical outline. The blue shaded region is the 'bag' representing 50% of the eruption centres when ranked by Tukey depth. The fence is the dashed black line, and red coloured triangles are outlier centres.

https://doi.org/10.5194/egusphere-2026-2684
Preprint. Discussion started: 13 July 2026

Analysis of the distance of the next eruption to the prior convex hull (Figure 6) shows two main trends. For ‘next’ eruptions outside the prior hull (shown in red), the distance is generally decreasing over time. However, for eruptions inside the hull (blue) the distance slightly increases over time.

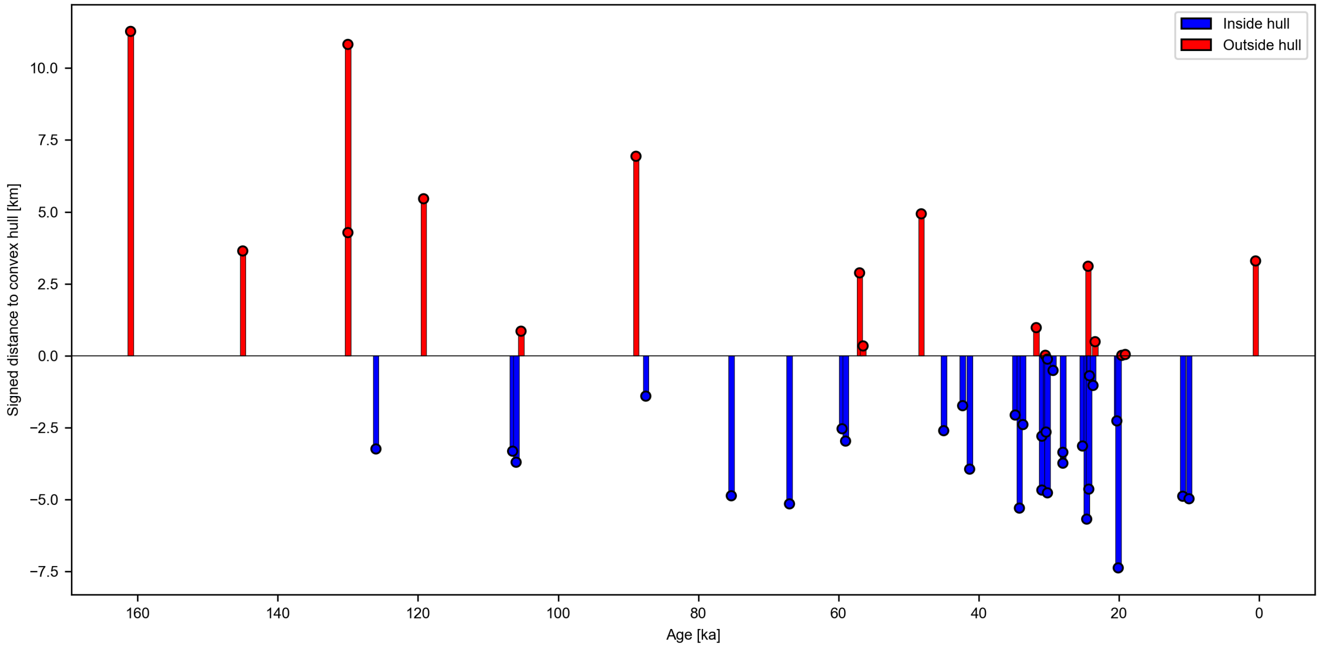

Figure 6. Distance of the ‘next’ eruption to the prior convex hull. Eruptions outside the convex hull are red, whilst those inside are blue.

The mean time gap of eruptions outside the convex hull is 10.0 ka (median = 9.7 ka) with a standard deviation of 8.7 ka, suggesting no narrow distribution of time ranges for how often an eruption occurs outside the field boundary.

3.2 Synthetic dataset

The synthetic dataset, which is based on 1000 simulations with 250 randomly located eruptive centres per simulation, allows us to examine scenarios of field growth and boundary evolution across a large number of eruptions and to place robust confidence limits on the analysis. The results, shown in Figure 7, reveal similar patterns to the AVF case study example. Simulations run with a larger bounding ellipse (adding 2 and 5 km buffers to the AVF ellipse) also show matching trends (Appendix Figure A1).

As the number of eruptions increases, the area ratio of the field (i.e. ratio between the convex hull and AVF ellipse area defined by Spörli and Eastwood (1997) increases logarithmically (Figure 7A). The observed AVF data follow a similar trend, although the values of the area ratios tend to be slightly higher than the synthetic ratios. This result is expected since the synthetic dataset has a known and absolute bounding ellipse, whereas the size of the AVF bounding ellipse considers only eruptions to date. The potential true size of the AVF bounding ellipse is unknown and theoretically larger than the estimate

https://doi.org/10.5194/egusphere-2026-2684
Preprint. Discussion started: 13 July 2026

of Spörli and Eastwood (1997) (e.g. Bebbington, 2013). Therefore, while the overall growth patterns in the observed data accurately represent the evolution of the field, the area ratio of the AVF data in Figure 7A is most certainly overestimated.

Similarly, the percentage of synthetic eruptive centres occurring within the preceding convex hull also increases logarithmically (Figure 7B) and, when eruptions do occur outside of the prior convex hull, their distance to the hull boundary progressively decreases with increasing eruption count (Figure 7C). The observed AVF data follow a similar trend in the distance outside of the previous hull, with all vents falling within the range defined by the synthetic dataset (Figure 7C). For the next (55th) AVF eruption, 22% of simulations produced eruptions outside of the prior hull (Figure 7B) with 95% of those eruptions occurring with 2.5 km of the convex hull boundary (Figure 7C).

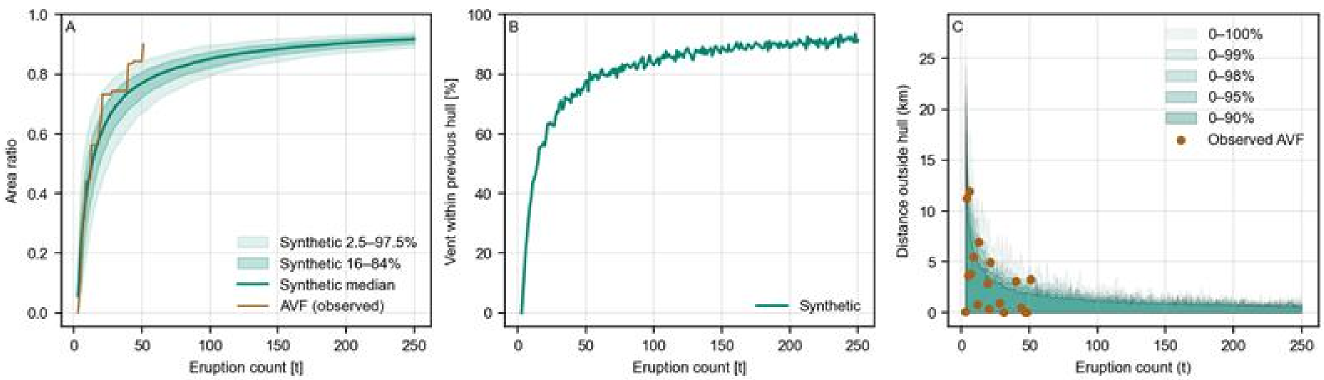

Figure 7. A) Ratio of the area of the convex hull to the AVF ellipse from Spörli and Eastwood (1997) for the synthetic dataset (green) and observed AVF data, brown. B) Percentage of synthetic eruptive centres within the preceding convex hull as a function of eruption number. C) Distances of eruptions that occurred outside of the convex hull to the hull boundary, as a function of eruption count. Various percentile ranges are shown as green shaded regions, with observed AVF data in brown points.

3.3 Clustering and alignment

The location of volcanic centres in the synthetic model simulations are randomly assigned, such that the distribution of distances between successive eruptions defines the null hypothesis to test whether vents within the AVF are also randomly distributed. Across the synthetic dataset, only 5% of vents occur within 2584 m of the preceding eruption. In contrast, excluding the first vent, 9 of the 50 vents (18%) in the AVF occur within 2584 m of the previous eruption, and are therefore considered to be spatially clustered (Figure 8A). The azimuthal trend between these clustered centres indicates a NNE/NE structural alignment (Figure 8B).

https://doi.org/10.5194/egusphere-2026-2684
Preprint. Discussion started: 13 July 2026

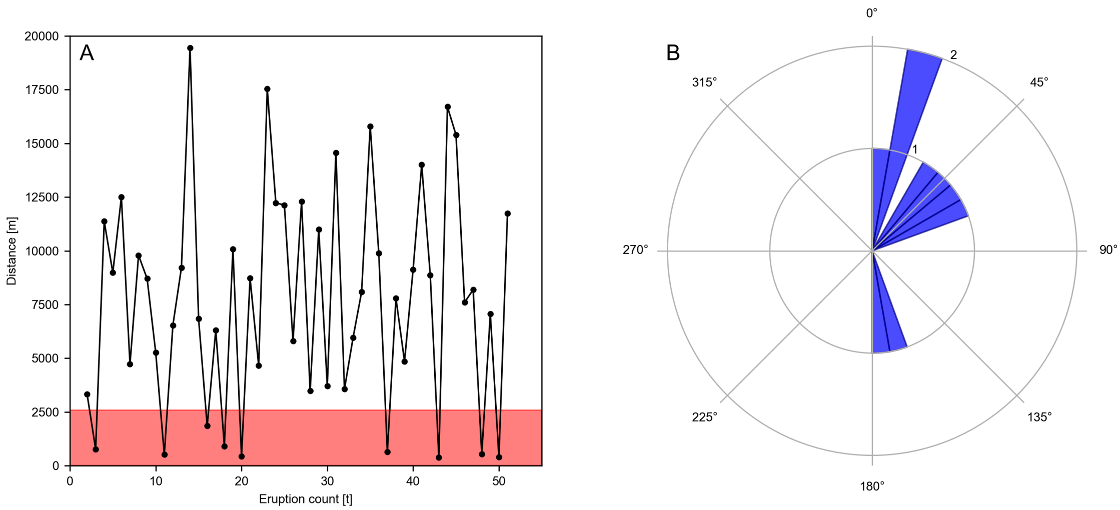

Figure 8. A) Distance between consecutive eruption centres. The shaded region reflects the lower 5th percentile of distances from the synthetic analysis. B) Spatial orientation of anomalously clustered vents showing a mostly NNE/NE alignment.

3.4 Eruption location probability relative to the field boundary

Using the dataset of 51 dated centres, and the first three eruptions to form the first convex hull, we find that 31 out of 48 eruption centres (i.e. 64%) were inside the previously existing boundary. However, the synthetic dataset demonstrates that as the volcanic field boundary evolves and expands over time, the probability of the next eruption occurring within the prior convex hull increases (Figure 7B). When only centres younger than 63 ka are considered (i.e. centres within the two younger time ranges illustrated in Figure 2), we find that 25 out of 35 eruption centres (i.e. 71%) were inside the previously existing boundary.

The Monte Carlo bootstrap analysis, that considers age uncertainty, shows that 65% of eruption centres (mean of the distribution) were inside the previously existing boundary. When centres younger than 63 ka are considered, 74% of eruptive centres (mean) were inside the previously existing boundary. This result is in good agreement with both the leave-one-out analysis, where 75% of left out eruptions were within the previous convex hull, and the synthetic dataset, where 74% of eruptive centres at t=52 occurred within the existing hull. This proportion increased to 78% for the 55th eruptive centre (i.e., the true ‘next’ eruption including undated vents).

3.5 Buffer distance and eruption location probability relative to the field boundary

As expected, the likelihood of an eruption occurring within the preceding convex hull increases with a larger buffer distance across all seven methods (Figure 9). However, the rate of increase varies between methods. For example, using the absolute eruptive chronology, more than 95% of eruptionsoccur within the previous convex hull with a buffer of 7 km (red), whereas the

https://doi.org/10.5194/egusphere-2026-2684
Preprint. Discussion started: 13 July 2026

required buffer drops to 5 km when age uncertainty is accounted for (purple). A buffer of 3.5 km is sufficient to capture 95% of young (i.e., <63 ka) eruptions using both the absolute chronology (blue) and when accounting for age uncertainty (green). The leave-one-out analysis shows slightly higher probabilities for different buffer distances, capturing 95% of eruptions with a buffer of 2 km when all data are considered (orange), and just 1 km when restricted to the young AVF eruptions (yellow). The synthetic dataset result for the 52nd AVF eruption is similar to the leave-one-out analysis, where 95 of eruptions are captured with a 1.5 km buffer (black).

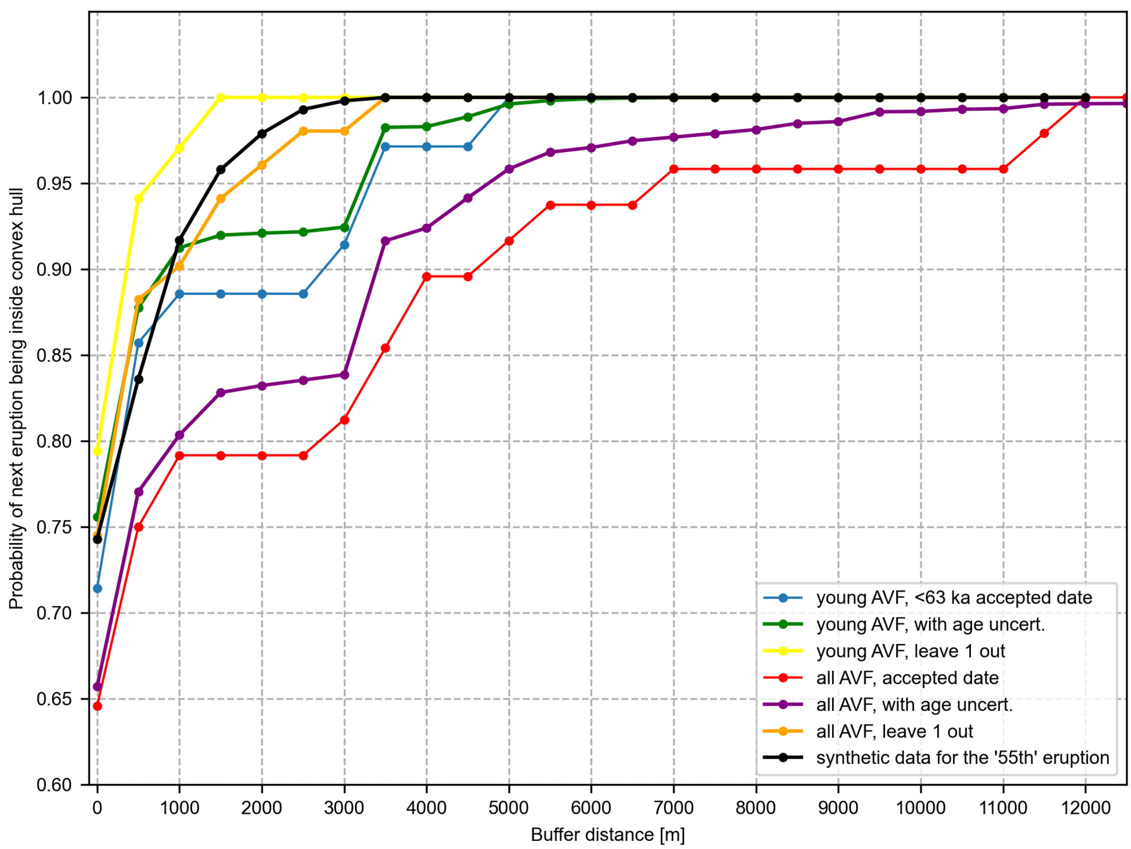

Figure 9. Probability of the next eruption being inside the previous boundary of the AVF as a function of the buffer distance for different age datasets. The red and blue curves are computed using the accepted age values for all eruption centres and those <63 ka respectively. The purple and green curves are the 97.5 percentile from Monte Carlo simulations of age uncertainty for all eruption centres and those <63 ka respectively. The orange and red curves are from the leave-one-out analysis for all eruption centres and those <63 ka respectively. The black curve is from the synthetic dataset for the next i.e., 55th AVF eruption.

https://doi.org/10.5194/egusphere-2026-2684
Preprint. Discussion started: 13 July 2026

4 Discussion

4.1 Spatio-temporal growth patterns in the AVF

To a first order, the broad distribution of volcanic centres in the AVF shows consistent patterns through time. Volcanic centres consistently fit a Poisson model over the course of the volcanic field's history, signifying that vent distributions are largely randomly positioned within the boundary ellipse of the field (Le Corvec et al. (2013b)). Indeed, our results show that at each areal growth step the spatial distribution of centres is largely random. For example, in the static areal change period between 88 and 59 ka, eruptions occurred from Maungauika [14] in the north of the field to Maungataketake [13] in the south (Figure 1). In this sense, the growth of the AVF closely matches the patterns observed from our model simulations (Figure 7), revealing that the likelihood of an eruption outside the convex hull and ideal buffer distance will decrease steadily with each successive eruption. Indeed, the observed AVF growth statistics generally follow the predicted model (Figure 7A), aside from the last 5 eruptions where the field area ratio to the AVF ellipse expands faster than predicted. The distance of the next eruption outside the convex hull shows more variance in the observed data (Figure 7C), but is still within the limits predicted by the synthetic data. Both these analyses confirm the largely random nature of AVF eruption locations.

However, closer inspection of spatio-temporal patterns in vent locations suggest some spatial clustering on shorter timescales. Nearly twenty percent of volcanic centres in the AVF occur within 2584 m of the previous centre (Figure 8). This value far exceeds the clustering observed in our synthetic dataset, where only 5% of eruptions occurred within 2584 m of the previous centre. Additionally, between 32 and 25 ka there was greater clustering of eruption centres in the south of the field around Te Manurewa-o-Tamapahore [31] and Crater Hill [32]; however, eruptions also occurred at Maungarahiri [39] in the centre of the field. On a larger scale there is a slight bias for eruptions in the southwest of the AVF within the 125 to 63 ka time interval (Figure 3B), whilst in the 63 to 15 ka time interval (panel C) the southeastern boundary of the field expanded via a series of new centres. Since approximately 100 ka the AVF has also expanded in a stepped fashion with clusters of eruptions within the field followed by an expansion of the field, and then another cluster of events within the enlarged boundaries (Figure 4). There is no clear time pattern to how often the field boundary expands.

The decreasing distance of next eruptions outside the convex hull (Figure 6) suggests that a physical limit exists on the magma source extent, such as that proposed by Spörli and Eastwood (1997). However, as the most recent eruption extended the hull extent, it remains to be seen if the field is entering a new paradigm with perhaps a shift of magma source, or whether the location of the most recent eruptions is just a reflection of the expected spatial variability of eruptive centres with the current AVF boundary ellipse.

Finer-scale temporal clustering of eruptive centres has been described previously for the AVF (Le Corvec et al., 2013a; Cassidy et al., 1999; Rout et al., 1993). Based on geochemical affinities between closely spaced vents and common anomalous paleomagnetic directions, this potential clustering was interpreted to reflect a shifting magma source through time (Le Corvec et al., 2013a), rather than vent clustering driven by pre-existing crustal pathways or changing stress regimes. However we suggest that, in addition to a shifting magma source, the stepped growth in areal extent could support the presence of preferred magma pathways that are created and utilised for a period of time until either the source location moves, or the pathway itself

https://doi.org/10.5194/egusphere-2026-2684
Preprint. Discussion started: 13 July 2026

becomes less viable due to factors such as a changing tectonic stress state or cooling and solidification of previous conduits. In support of this hypothesis we observe a distinct NNE to NE bias for spatio-temporally clustered centres (Figure 8), where 7 out of 9 of the clustered eruptions erupted to the NNE/NE of the initial eruption, which may also reflect the presence of short-term preferred structural pathways that remain viable for more than one eruption.

4.2 Will the next AVF eruption occur within the present convex hull boundary?

Results presented here provide important considerations for emergency planning associated with volcanic crises in the AVF, and similar volcanic fields globally. Across the last 63 kyrs 71% of AVF eruptions have occurred within the existing convex hull, increasing to ∼98% when a 3.5 km buffer is added (Figure 9). All dated young AVF eruptions (Figure 9 blue and green lines) occurred within a 5 km buffer of the existing convex hull, which was a qualitative buffer developed by Runge et al. (2014), lending quantitative weight supporting continued use of a 5 km buffer for planning for a future event.

However, it is important to distinguish between retrospective and predictive approaches. Estimates using the absolute and bootstrapped chronologies are retrospective; they reveal how often eruptions fell within a boundary defined by earlier vents across the full (or at least partial) eruptive record. However, the synthetic dataset demonstrates that the probability of an eruption occurring within the convex hull increases logarithmically with eruption count (Figure 9), so the retrospective approaches are inherently biased toward lower probabilities and larger buffer distances. As such, they provide the most conservative constraints on both eruption likelihood within the field and required buffer size.

In contrast, the leave-one-out analysis provides insight into the most recent eruption, while the synthetic dataset evaluates the location of the ‘next’ eruption. These predictive approaches yield higher probabilities that the next eruption will occur within the existing hull (75% and 74%, respectively) and smaller buffer distances, suggesting that a 2 km buffer is sufficient to capture at least 95% of future eruptions.

The logarithmic nature of the probability increase compared to buffer distance, means that the 5 km buffer offers only a few percent (<3%) extra confidence for the trade off of a 43% increase in buffer size compared to a 3.5 km buffer, or 150% increase in buffer size compared to a 2 km buffer. It is also important to note that our calculated buffers do not account for the impacts of hazards such as lava flow, ash fall or base surges that may emanate from the eruption centre location and extend beyond these buffer distances.

5 Conclusions

Here we outline a method to examine the likelihood that next eruption occurring at a monogenetic volcanic field will be within the convex hull of the existing eruption centres. The method is based on the proportion of ‘next’ eruptions occurring within the evolving field boundary over its lifespan and was applied to the well-dated Auckland Volcanic Field, New Zealand. The areal extent of the AVF field is shown to have grown steadily through time in a step-wise fashion with some spatio-temporal clustering of eruptive centres. Highly clustered successive eruption centres (within 2584 m of the previous) are aligned to the

https://doi.org/10.5194/egusphere-2026-2684
Preprint. Discussion started: 13 July 2026

NNE/NE, suggesting structural control on magma pathways and that established pathways may remain viable for some time interval after an eruption.

Analysis of the observed AVF data over the last 63 kyrs indicates that 71% of eruptions (or 74% when age uncertainty is considered) have occurred within the preceding convex hull. However, the forward-looking synthetic dataset demonstrates that this probability is not static but rather increases logarithmically through time. Analysis of the synthetic data set suggests there is a 74 -75% probability that the next vent will fall within the existing convex hull, and that a 2 km buffer is sufficient to increase that likelihood to 98%. Analysis of the observed data is slightly more conservative and suggests that a 3.5 km buffer is sufficient to increase that likelihood to >95%. It reaches virtually 100% at 5 km, supporting continued use of the 5km Runge et al. (2014) buffer as the most conservative distance for planning for a future event.

Finally, we recommend that future dating efforts focus on reducing the uncertainty of age dates with large errors and obtaining ages for the remaining undated eruption centres.

Code and data availability. The dataset used is available from Hopkins et al. (2021) and Miller et al. (2026). The code to reproduce analyses and figures is available from https://github.com/craigmillernz/AVF_boundary_evolution_paper.

Video supplement. An animated GIF of the Auckland Volcanic Field growth is available at Miller et al. (2026)

Appendix A

Figure A1 shows synthetic models using the AVF ellipse size of Spörli and Eastwood (1997) and the effect of increasing that ellipse by two and five kilometres.

https://doi.org/10.5194/egusphere-2026-2684
Preprint. Discussion started: 13 July 2026

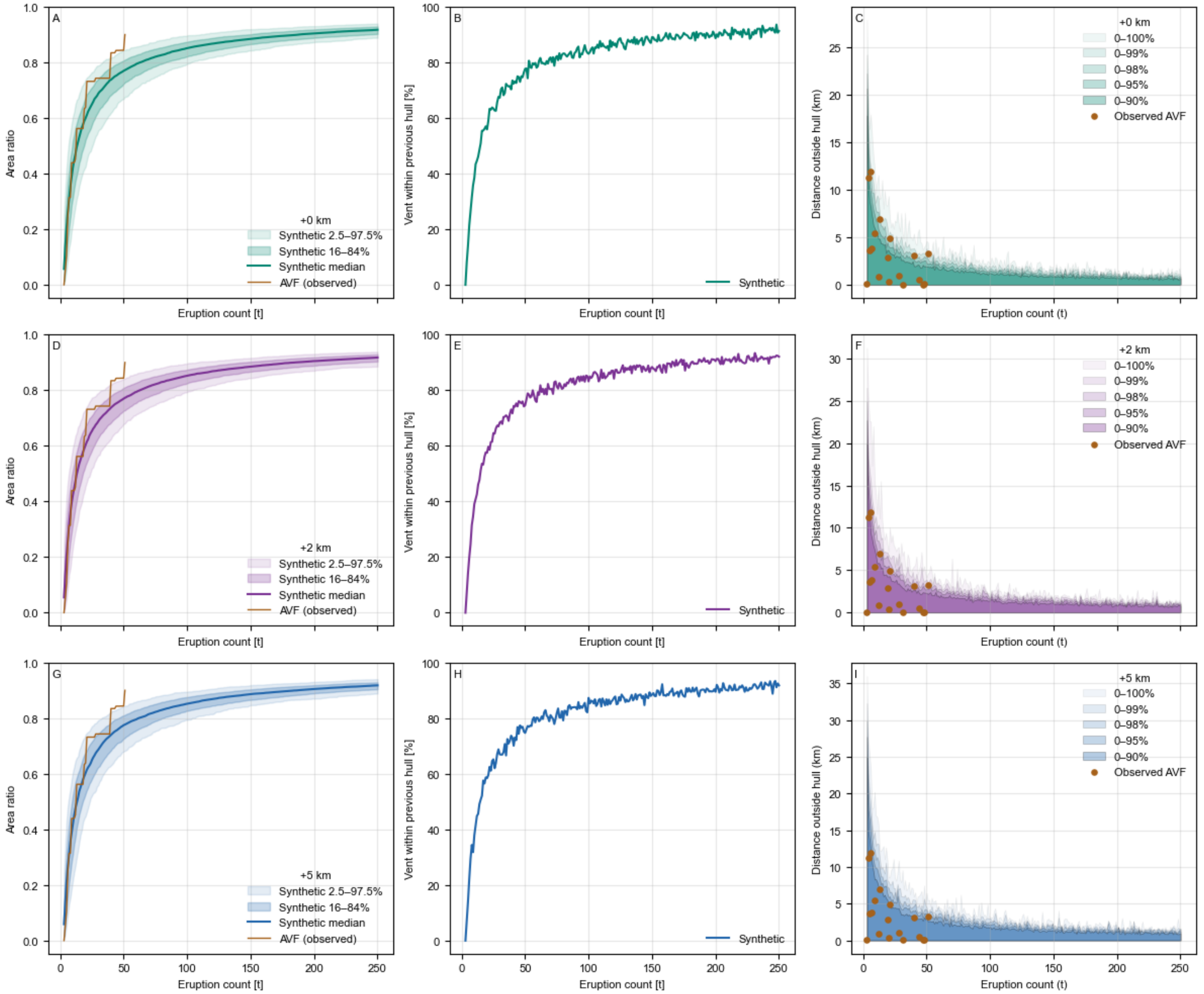

Figure A1. Synthetic models of the AVF run for different size ellipses. A-C) As per Figure 7, D-F) AVF ellipse + 2 km, G-I) AVF ellipse + 5km. Panels A,D,G show the area ratio of the ellipse to the convex hull for each eruption. Panels B,E,H show the percentage of vents outside the hull. Panels C,F,I show the distance outside the convex hull for each eruption.

Author contributions. C.M. conceived the study, undertook the initial analysis and wrote the first draft of the paper. J.M., E.J., D.T., A.D.,
325 G.L. and J.L. contributed to data analysis, writing and editing.

https://doi.org/10.5194/egusphere-2026-2684
Preprint. Discussion started: 13 July 2026

Competing interests. The authors declare no competing interests are present.

Acknowledgements. This study was in part funded by the Natural Hazards Commission Toka Tū Ake and Auckland Council through the DEtermining VOlcanic Risk in Auckland (DEVORA) research programme. We thank the organisers and participants of the 2025 DEVORA Forum that stimulated this work.

https://doi.org/10.5194/egusphere-2026-2684
Preprint. Discussion started: 13 July 2026

References

Allen, S. and Smith, I. E.: Eruption Styles and Volcanic Hazard in the Auckland Volcanic Field, New Zealand, Geoscience Reports Shizuoka Univ., 20, 5–14, 1994.

Allington, M. L., Nilsson, A., Hill, M. J., Suttie, N., Daniil, D., Hjorth, I., Aulin, L., Augustinus, P. C., and Shane, P.: Constraining the Eruption History of Rangitoto Volcano, New Zealand, Using Palaeomagnetic Data, Quaternary Geochronology, 78, 101 459, https://doi.org/10.1016/j.quageo.2023.101459, 2023.

Ang, P. S., Bebbington, M. S., Lindsay, J. M., and Jenkins, S. F.: From Eruption Scenarios to Probabilistic Volcanic Hazard Analysis: An Example of the Auckland Volcanic Field, New Zealand, Journal of Volcanology and Geothermal Research, 397, 106 871, https://doi.org/10.1016/j.jvolgeores.2020.106871, 2020.

Auckland Council: Tāmaki Makaurau Auckland Civil Defence Emergency Management Group Plan 2024-2029, Tech. rep., Auckland Council, New Zealand, ISBN 978-1-991146-32-8 (Print), 978-1-991146-33-5 (PDF), 2024.

Auckland Emergency Management: Auckland Volcanic Field Response Plan, Tech. Rep. 1.00, 2024.

Bebbington, M. S.: Assessing Spatio-Temporal Eruption Forecasts in a Monogenetic Volcanic Field, Journal of Volcanology and Geothermal Research, 252, 14–28, https://doi.org/10.1016/j.jvolgeores.2012.11.010, 2013.

Bebbington, M. S. and Cronin, S. J.: Spatio-Temporal Hazard Estimation in the Auckland Volcanic Field, New Zealand, with a New Event-Order Model, Bulletin of Volcanology, 73, 55–72, https://doi.org/10.1007/s00445-010-0403-6, 2011.

Bebbington, M. S., Whitehead, M. G., and Kereszturi, G.: Brief Communication: A Magma Depletion Alternative for Vent Distribution in Volcanic Fields, Natural Hazards and Earth System Sciences, 25, 3455–3460, https://doi.org/10.5194/nhess-25-3455-2025, 2025.

Brenna, M., Cronin, S. J., Smith, I. E. M., Sohn, Y. K., and Maas, R.: Spatio-Temporal Evolution of a Dispersed Magmatic System and Its Implications for Volcano Growth, Jeju Island Volcanic Field, Korea, Lithos, 148, 337–352, https://doi.org/10.1016/j.lithos.2012.06.021, 2012.

Cañón-Tapia, E.: Reappraisal of the Significance of Volcanic Fields, Journal of Volcanology and Geothermal Research, 310, 26–38, https://doi.org/10.1016/j.jvolgeores.2015.11.010, 2016.

Cañón-Tapia, E.: Geological Significance of the Spatial Clustering and Alignment of Vents in Zones of Distributed Volcanism: A Critical Review, Boletín de la Sociedad Geológica Mexicana, 75, https://doi.org/10.18268/bsgm2023v75n3a130923, 2023.

Cassidy, J., Locke, C. A., Miller, C. A., and Rout, D. J.: The Auckland Volcanic Field, New Zealand: Geophysical Evidence for Its Eruption History, Geological Society, London, Special Publications, 161, 1–10, https://doi.org/10.1144/GSL.SP.1999.161.01.02, 1999.

Connor, C. B., Condit, C. D., Crumpler, L. S., and Aubele, J. C.: Evidence of Regional Structural Controls on Vent Distribution: Springerville Volcanic Field, Arizona, Journal of Geophysical Research: Solid Earth, 97, 12 349–12 359, https://doi.org/10.1029/92JB00929, 1992.

Dahm, T., Stiller, M., Mechie, J., Heimann, S., Hensch, M., Woith, H., Schmidt, B., Gabriel, G., and Weber, M.: Seismological and Geophysical Signatures of the Deep Crustal Magma Systems of the Cenozoic Volcanic Fields Beneath the Eifel, Germany, Geochemistry, Geophysics, Geosystems, 21, e2020GC009 062, https://doi.org/10.1029/2020GC009062, 2020.

Global Volcanism Program: Volcanoes of the World, https://doi.org/10.5479/si.GVP.VOTW5-2025.5.3, 2025-11-26, 2025.

Hayes, J., Tsang, S., Fitzgerald, R., Blake, D. M., Deligne, N. I., Doherty, A., Hopkins, J. L., Hurst, A. W., Le Corvec, N., Leonard, G. S., Lindsay, J., Miller, C. A., Nemeth, K., Smid, E. R., White, J., and Wilson, C. J. N.: The DEVORA Scenarios: Multi-Hazard Eruption Scenarios for the Auckland Volcanic Field, Tech. Rep. 29, GNS Science, 2018.

Heron, D.: Geological Map of New Zealand 1:250 000., https://doi.org/10.21420/5XTJ-5718, 2023.

https://doi.org/10.5194/egusphere-2026-2684
Preprint. Discussion started: 13 July 2026

Hopkins, J. L., Smid, E. R., Eccles, J. D., Hayes, J. L., Hayward, B. W., McGee, L. E., van Wijk, K., Wilson, T. M., Cronin, S. J., Leonard, G. S., Lindsay, J. M., Németh, K., and Smith, I. E. M.: Auckland Volcanic Field Magmatism, Volcanism, and Hazard: A Review, New Zealand Journal of Geology and Geophysics, 64, 213–234, https://doi.org/10.1080/00288306.2020.1736102, 2021.

Kereszturi, G., Németh, K., Cronin, S. J., Agustín-Flores, J., Smith, I. E. M., and Lindsay, J.: A Model for Calculating Eruptive Volumes for Monogenetic Volcanoes — Implication for the Quaternary Auckland Volcanic Field, New Zealand, Journal of Volcanology and Geothermal Research, 266, 16–33, https://doi.org/10.1016/j.jvolgeores.2013.09.003, 2013.

Le Corvec, N., Bebbington, M. S., Lindsay, J. M., and McGee, L. E.: Age, Distance, and Geochemical Evolution within a Monogenetic Volcanic Field: Analyzing Patterns in the Auckland Volcanic Field Eruption Sequence, Geochemistry, Geophysics, Geosystems, 14, 3648–3665, https://doi.org/10.1002/ggge.20223, 2013a.

Le Corvec, N., Spörli, K. B., Rowland, J., and Lindsay, J.: Spatial Distribution and Alignments of Volcanic Centers: Clues to the Formation of Monogenetic Volcanic Fields, Earth-Science Reviews, 124, 96–114, https://doi.org/10.1016/j.earscirev.2013.05.005, 2013b.

Leonard, G. S., Calvert, A. T., Hopkins, J. L., Wilson, C. J., Smid, E. R., Lindsay, J. M., and Champion, D. E.: High-Precision 40Ar/39Ar Dating of Quaternary Basalts from Auckland Volcanic Field, New Zealand, with Implications for Eruption Rates and Paleomagnetic Correlations, Journal of Volcanology and Geothermal Research, 343, 60–74, https://doi.org/10.1016/j.jvolgeores.2017.05.033, 2017.

Lindsay, J., Marzocchi, W., Jolly, G., Constantinescu, R., Selva, J., and Sandri, L.: Towards Real-Time Eruption Forecasting in the Auckland Volcanic Field: Application of BET_EF during the New Zealand National Disaster Exercise 'Ruaumoko', Bulletin of Volcanology, 72, 185–204, https://doi.org/10.1007/s00445-009-0311-9, 2010.

Lindsay, J. M., Smid, E. R., Balfour, N., Deligne, N. I., Doherty, A., Hall, A., Howe, T., Jolly, G., Leonard, G., Lewis, K., Miller, C. A., Ema Nersezova, Roberts, R., Smith, R. E., Stolberger, T., Tapuke, K., and Wilson, T. M.: Determining Volcanic Risk in Auckland (DEVORA) Research Programme—A Transdisciplinary Approach to Address the Challenge of Distributed Volcanism in an Urban Environment, Tech. Rep. 1890-B, U.S. Geological Survey, ISSN 2330-7102, https://doi.org/10.3133/pp1890B, 2026.

Lindsay, JM., Leonard, GS., Smid, ER., and Hayward, BW.: Age of the Auckland Volcanic Field: A Review of Existing Data, New Zealand Journal of Geology and Geophysics, 54, 379–401, https://doi.org/10.1080/00288306.2011.595805, 2011.

Linnell, T., Shane, P., Smith, I., Augustinus, P., Cronin, S., Lindsay, J., and Maas, R.: Long-Lived Shield Volcanism within a Monogenetic Basaltic Field: The Conundrum of Rangitoto Volcano, New Zealand, Bulletin of the Geological Society of America, 128, 1160–1172, https://doi.org/10.1130/B31392.1, 2016.

Magill, C. R., McAneney, K. J., and Smith, I. E. M.: Probabilistic Assessment of Vent Locations for the Next Auckland Volcanic Field Event, Mathematical Geology, 37, 227–242, https://doi.org/10.1007/s11004-005-1556-2, 2005.

Marrero, J. M., García, A., Berrocoso, M., Llinares, Á., Rodríguez-Losada, A., and Ortiz, R.: Strategies for the Development of Volcanic Hazard Maps in Monogenetic Volcanic Fields: The Example of La Palma (Canary Islands), Journal of Applied Volcanology, 8, 6, https://doi.org/10.1186/s13617-019-0085-5, 2019.

Martí, J., López, C., Bartolini, S., Becerril, L., and Geyer, A.: Stress Controls of Monogenetic Volcanism: A Review, Frontiers in Earth Science, 4, https://doi.org/10.3389/feart.2016.00106, 2016.

Mazzarini, F. and Isola, I.: The Spatial Distribution and Evolution of Volcanic Vents in Monogenetic Fields in Active Extensional Tectonic Setting: Examples from the Northern Main Ethiopian Rift (Ethiopia), Journal of Volcanology and Geothermal Research, 451, 108 093, https://doi.org/10.1016/j.jvolgeores.2024.108093, 2024.

Mazzarini, F., Le Corvec, N., Isola, I., and Favalli, M.: Volcanic Field Elongation, Vent Distribution, and Tectonic Evolution of a Continental Rift: The Main Ethiopian Rift Example, Geosphere, 12, 706–720, https://doi.org/10.1130/GES01193.1, 2016.

https://doi.org/10.5194/egusphere-2026-2684
Preprint. Discussion started: 13 July 2026

Miller, C., Muirhead, J. D., Judd, E. J., Townsend, D., Lindsay, J. M., and Leonard, G. S.: Evolution of the Auckland Volcanic Field (New Zealand) Boundary, https://doi.org/10.5281/zenodo.19688038, 2026.

Needham, A., Lindsay, J., Smith, I., Augustinus, P., and Shane, P.: Sequential Eruption of Alkaline and Sub-Alkaline Magmas from a Small Monogenetic Volcano in the Auckland Volcanic Field, New Zealand, Journal of Volcanology and Geothermal Research, 201, 126–142, https://doi.org/10.1016/j.jvolgeores.2010.07.017, 2011.

Németh, K. and Kereszturi, G.: Monogenetic Volcanism: Personal Views and Discussion, International Journal of Earth Sciences, 104, 2131–2146, https://doi.org/10.1007/s00531-015-1243-6, 2015.

Rousseeuw, P. J. and Ruts, I.: Bagplot: A Bivariate Boxplot, The American Statistician, 53, 382–387, 1999.

Rout, D. J., Cassidy, J., Locke, C. A., and Smith, I. E. M.: Geophysical Evidence for Temporal and Structural Relationships within the Monogenetic Basalt Volcanoes of the Auckland Volcanic Field, Northern New Zealand, Journal of Volcanology and Geothermal Research, 57, 71–83, https://doi.org/10.1016/0377-0273(93)90032-M, 1993.

Runge, M. G., Bebbington, M. S., Cronin, S. J., Lindsay, J. M., Kenedi, C. L., and Moufti, M. R. H.: Vents to Events: Determining an Eruption Event Record from Volcanic Vent Structures for the Harrat Rahat, Saudi Arabia, Bulletin of Volcanology, 76, 804, https://doi.org/10.1007/s00445-014-0804-z, 2014.

Runge, M. G., Bebbington, M. S., Cronin, S. J., Lindsay, J. M., and Moufti, M. R.: Sensitivity to Volcanic Field Boundary, Journal of Applied Volcanology, 4, 22, https://doi.org/10.1186/s13617-015-0040-z, 2015.

Shane, P., Gehrels, M., Zawalna-Geer, A., Augustinus, P., Lindsay, J., and Chaillou, I.: Longevity of a Small Shield Volcano Revealed by Crypto-Tephra Studies (Rangitoto Volcano, New Zealand): Change in Eruptive Behavior of a Basaltic Field, Journal of Volcanology and Geothermal Research, 257, 174–183, https://doi.org/10.1016/j.jvolgeores.2013.03.026, 2013.

Smith, I. E. M. and Németh, K.: Source to Surface Model of Monogenetic Volcanism: A Critical Review, in: Monogenetic Volcanism, edited by Németh, K., Carrasco-Núñez, G., Aranda-Gómez, J. J., and Smith, I. E. M., vol. 446, p. 0, Geological Society of London, ISBN 978-1-78620-283-3, https://doi.org/10.1144/SP446.14, 2017.

Spörli, B. K. and Eastwood, V. R.: Elliptical Boundary of an Intraplate Volcanic Field, Auckland, New Zealand, Journal of Volcanology and Geothermal Research, 79, 169–179, https://doi.org/10.1016/S0377-0273(97)00030-9, 1997.

Tadini, A., Bonali, F. L., Corazzato, C., Cortés, J. A., Tibaldi, A., and Valentine, G. A.: Spatial Distribution and Structural Analysis of Vents in the Lunar Crater Volcanic Field (Nevada, USA), Bulletin of Volcanology, 76, 877, https://doi.org/10.1007/s00445-014-0877-8, 2014.

Torres, A. N., Del Pozzo, A. L. M., Groppelli, G., and del Carmen Jaimes Viera, M.: Risk Scenarios for a Future Eruption in the Chichinautzin Monogenetic Volcanic Field, South México City, Journal of Volcanology and Geothermal Research, 433, 107 733, https://doi.org/10.1016/j.jvolgeores.2022.107733, 2023.

Tukey, J. W.: Mathematics and the Picturing of Data, in: Proceedings of the International Congress of Mathematicians, vol. 2, pp. 523–531, Canadian Mathematical Congress, 1975.

Zhang, R., Yagolnitzer, Y., Brenna, M., White, J. D. L., Kereszturi, G., Wang, T., and Hemming, S. R.: Spatiotemporal Development of Diverse Magmatic Plumbing in Long-Lived Distributed Volcanic Fields, Bulletin of Volcanology, 87, 70, https://doi.org/10.1007/s00445-025-01859-4, 2025.